

Research Article

Time Delay Compensation for Tracking Differentiator and Its Application on Phase Sensor

Fengshan Dou, Song Xue and Dapeng Zhang

Department of Mechatronics Engineering and Automation, National University of Defense Technology, Changsha 410073, China

Abstract: This study shows the time delay compensation for tracking differentiator and its application on phase sensor. Filtering time delay compensation algorithm for phase sensor of high speed maglev train with Electromagnetic Suspension (EMS) system is studied. Firstly, the structure and functions of the sensor are introduced. Secondly, the reasons for the phase signal distortion are analyzed. Then, a kind of nonlinear Tracking Differentiator (TD) is introduced. The time delay characteristics of the nonlinear TD are studied and the time delay constant is figured out approximately. Then, a compensation algorithm is proposed based on phase forecasting. At last the TD and its compensation algorithms are applied to the phase signal to improve the waveform. The experimental results show that the designed algorithm is effective.

Keywords: Maglev train, phase detection, time delay compensation, tracking differentiator

INTRODUCTION

The carriage of high speed maglev train with Electromagnetic Suspension (EMS) system is shown in Fig. 1.

The traction system of the train is based on the principle of linear synchronous motor (Liu, 1995; Wu, 2003; Long *et al.*, 2011a; Long *et al.*, 2011b). The long stator made of laminated silicon-steel sheets is fixed along the rail and three phased primary windings are embedded in the slots of the long stator. The suspension electromagnets are the secondary windings. In order to reach the most efficient and stable traction performance, the traction system needs to control the current phase of the primary windings to make the traveling magnetic field be synchronized with the secondary magnetic field. In this process, the precise phase information of the secondary windings is necessary.

Usually, magnetic-resistance type sensor is designed to find out the secondary phase by detecting the tooth-slot structure of the long stator based on nondestructive examination technology (Barandiaran and Kurlyandskaya, 2009; Thomas *et al.*, 2009). Some references propose solutions to realize the basic functions of the phase sensor for maglev train. Reference researches on the filtering algorithm for the phase signal based on Tracking Differentiator (TD) and resolve the time delay problem of the TD by multi-stage filtering and information fusion. But the calculation load of the time delay compensation algorithm designed in reference is somewhat big.

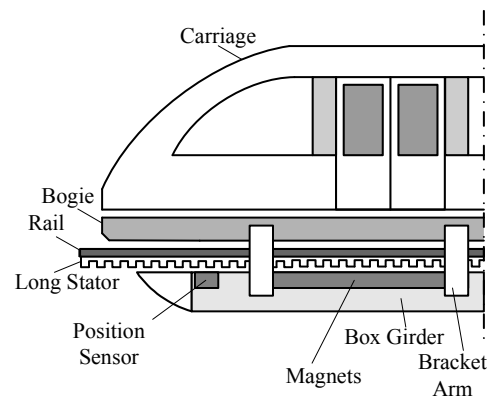


Fig. 1: The carriage of high speed maglev train

This study shows the time delay problem of phase signal filtering and proposes an effective compensation algorithm with relatively small computation needs.

METHODOLOGY

Operating principle of the phase sensor: There is a detecting coil fixed on one side of the sensor faced to the long stator. The resonance circuit of the coil is stimulated by a signal source with a constant frequency. When the coil moves with a uniform speed along the long stator at a constant suspension gap, its equivalent inductance changes periodically because of the tooth-slot structure and the signal amplitude of the resonance circuit fluctuates accordingly to form an amplitude-modulated signal. Through demodulation, an

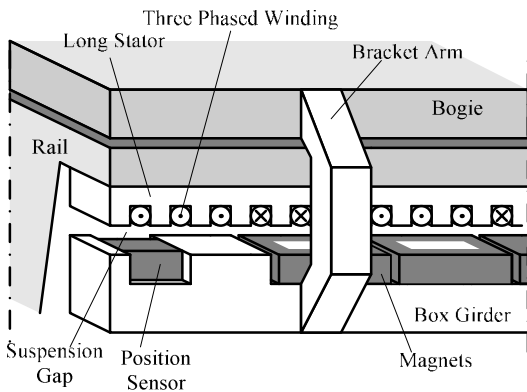


Fig. 2: The substructure of high speed maglev train

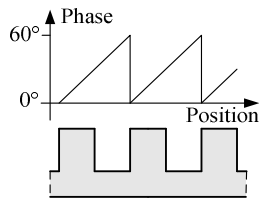


Fig. 3: The relationship between secondary phase and tooth-slot structure

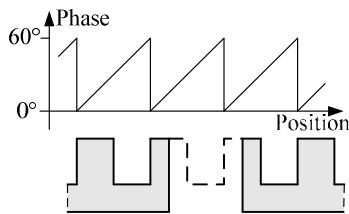


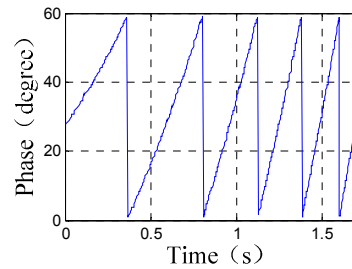
Fig. 4: The phase waveform requirement near a joint gap

approximated sine wave can be gotten. According to the sampled value of the sine wave, the precise secondary phase can be found out by table-lookup method. A magnetic pole phase period of the 3-phased windings contains 6 tooth-slot periods shown in Fig. 2. Thus, the length of a tooth-slot period is corresponding to an electrical angle of 60° shown in Fig. 3.

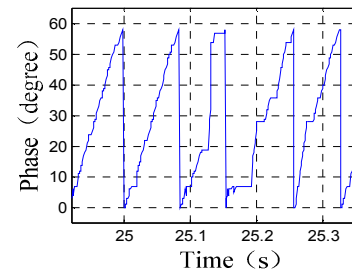
Then, a square wave can be gotten by putting the sine signal into a comparator. Thus, the tooth-slot period number can be gotten by counting the jumping edges of the square wave.

Thomas *et al.* (2009) study the table-lookup algorithm and suspension gap fluctuation compensation algorithm for the sensor to improve its performance. However, there are still some problems need to be considered:

- The suspension gap fluctuation compensation algorithm is invalid to high frequency fluctuation.



(a)



(b)

Fig. 5: Contrast of (a) normal phase signal, (b) distorted signal

It also amplifies noises and errors when the suspension gap is too large.

- There are joint gaps between certain long stator sections. The phase signal will be distorted seriously when the sensor is above a joint gap because there is no silicon-steel tooth-slot structure. But the traction system still requires normal phase signal in this situation, shown in Fig. 4.

The contrast of normal phase signal and distorted signal is shown in Fig. 5. The signals are collected during a test run and the distorted signal is collected near a joint gap.

Nonlinear TD: Classical differentiation element (Fig. 6a) using an inertia element $1/(ts + 1)$ to simulate time delay has serious noise amplifying effect. In order to improve noise restrain ability, second order differentiation element is proposed through introducing in two inertia elements shown in Fig. 6b. Where, $\tau_2 > \tau_1 > 0$.

Usually, τ_1 and τ_2 approximate a constant τ . So, the transfer function of second order differentiation element can be written as follows:

$$T(s) = \frac{r^2 s}{s^2 + 2rs + r^2}, r = \frac{1}{\tau} \quad (1)$$

The discrete state equations corresponding to (1) are:

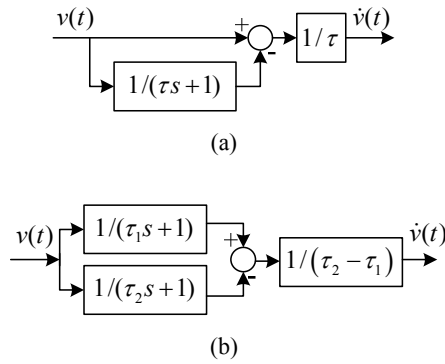


Fig. 6: Linear differentiation elements, (a) classical differentiation element, (b) second order differentiation element

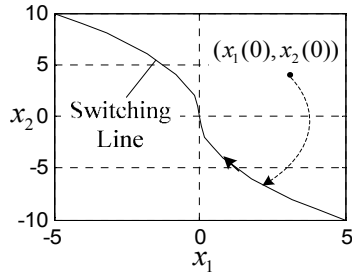


Fig. 7: State trajectory of system (3) and (4)

$$\begin{cases} x_1(k+1) = x_1(k) + hx_2(k) \\ x_2(k+1) = x_2(k) + h\{-r^2[x_1(k) - v(k)] - 2rx_2(k)\} \end{cases} \quad (2)$$

In system (2), $x_1(k)$ can track the input signal $v(k)$. $x_1(k)$ will be closer to $v(k)$, if r is bigger. In this case, $x_2(k)$ is the approximate value of $\dot{v}(k)$. Because of the tracking and differentiating function, systems having similar dynamic structure to system (2) are called Tracking Differentiator (TD). However, the noise suppression ability of linear TD still cannot satisfy the requirements of many practical signal processing applications.

Thus, considering nonlinear control system:

$$\begin{cases} \dot{x}_1 = x_2 \\ \dot{x}_2 = ru, |u| \leq 1, r > 0 \end{cases} \quad (3)$$

According to optimum control theory, the control law to make the system state move to the original point from any initial state in the shortest time is shown in (4):

$$u(t) = -\text{sign}(x_1(t) + x_2(t)|x_2(t)|/2r) \quad (4)$$

Driving by control law (4), the system state firstly moves to the control law switching line: $x_1(t) + x_2(t)$

$|x_2(t)|/2r = 0$ and then moves to the original point along the switching line shown in Fig. 7.

By substituting $x_1(t)-v(t)$ for $x_1(t)$ in Eq. (4) and then substituting Eq. (4) into (3), a nonlinear tracking differentiator is gotten as follows:

$$\begin{cases} \dot{x}_1 = x_2 \\ \dot{x}_2 = -r \text{sign}(x_1 - v + x_2|x_2|/2r) \end{cases} \quad (5)$$

For digital signal processing applications, a discrete form of system (5) is needed. But conventional discretization methods may bring in bad dynamic characteristics. Barandiaran and Kurlyandskaya (2009) do some researches on this problem and propose a discrete form of system (5) without reducing its dynamic performance as follows:

$$\begin{cases} x_1(k+1) = x_1(k) + hx_2(k) + rh^2u(k)/2 - b(k)h^3/3 \\ x_2(k+1) = x_2(k) + rhu(k) - b(k)h^2/2 \end{cases} \quad (6)$$

where,

h : The discretization time step length

$u(k)$ and $b(k)$ are calculated according to the following rules:

- If state $(x_1(k), x_2(k))$ is not on the switching line, let t_A denote the time span for the state to reach the switching line; if it is already on the switching line, let t_B denote the time span for the state to reach the original point. t_A and t_B are calculated as follows:

$$t_A = sx_2/r + \sqrt{sx_1/r + x_2^2/(2r^2)} \quad (7)$$

$$t_B = |x_2|/r \quad (8)$$

where,

$$s = \text{sign}(x_1 + x_2|x_2|/2r)$$

- If state $(x_1(k), x_2(k))$ is not on the switching line and $t_A \geq h$, then:

$$\begin{cases} b = 0 \\ u(k) = -s(k) \end{cases} \quad (9)$$

- If $t_A < h$, then:

$$\begin{cases} b = 0 \\ u(k) = -s(k)\left(-\frac{1}{2} + \frac{x_2(k)s(k)}{rh} + \frac{1}{2}\left(1 + \frac{4s(k)}{rh}(x_2(k) + \frac{2x_1(k)}{h})^{1/2}\right)\right) \end{cases} \quad (10)$$

- If $(x_1(k), x_2(k))$ is already on the switching line and $t_B \geq h$, then:

$$\begin{cases} b = 0 \\ u(k) = -\text{sign}(x_2(k)) \end{cases} \quad (11)$$

- If $t_B < h$, then:

$$\begin{cases} u(k) = a + bh \\ b = 6(x_2(k)h + 2x_1(k))/(rh^3) \\ a = -2(2x_2(k)h + 3x_1(k))/(rh^2) \end{cases} \quad (12)$$

After substituting $x_1(k)-v(k)$ for $x_1(k)$ and substituting $c_0 h$ for h in rules 1), 2) and 3), $x_1(k)$ can track and smooth the input signal $v(k)$ and $x_2(k)$ is the approximate value of $\dot{v}(k)$. c_0 is called as filtering factor. The bigger c_0 is, the smoother $x_1(k)$ is and the bigger the time delay of $x_1(k)$ is.

Time delay compensation for TD: The TD possesses low-pass filtering characteristics. It can reach its best filtering performance, if the frequency band of the input signal is much lower than a certain limit denoted by ω_0 which will be figured out later. In this case, t_A always satisfies $t_A < c_0 h$. And usually, because $v(k)$ is changing, $(x_1(k)-v(k), x_2(k))$ can't reach the switching line.

Most signals in engineering practice can be expressed by the linear combination or integral of sinusoidal signals with different frequencies. Thus, a sinusoidal signal is chosen as the input signal to study the time delay characteristics of nonlinear TD (6). Suppose the input signal before discretization is:

$$v(t) = A \sin(\omega t), \omega \ll \omega_0 \quad (13)$$

According to the discussion above, only the situation when $t_A < c_0 h$ is considered. Because usually a very big value can be assigned to r , the following in equation can be satisfied:

$$\frac{4s(k)}{rc_0h} \left(x_2(k) + \frac{2(x_1(k) - v(k))}{c_0h} \right) \ll 1 \quad (14)$$

Thus, according to Taylor's formula, the first order approximation of $u(k)$ in (10) is:

$$\begin{aligned} u(k) &\approx -s(k) \left(-\frac{1}{2} + \frac{x_2(k)s(k)}{rc_0h} \right. \\ &\quad \left. + \frac{1}{2} \left(1 + \frac{2s(k)}{rc_0h} \left(x_2(k) + \frac{2(x_1(k) - v(k))}{c_0h} \right) \right) \right) \quad (15) \\ &= -\frac{2x_2(k)}{rc_0h} - \frac{2(x_1(k) - v(k))}{r(c_0h)^2} \end{aligned}$$

In order to figure out the time delay constant τ , one way is to find out the approximate continuous signal $x_1(t)$ corresponding to $x_1(k)$ and then compare $x_1(t)$ with $v(t)$. So, substitute Eq. (15) and $b = 0$ into Eq. (6) and

then convert system (6) to its corresponding continuous system approximately shown in (16). When h is small and c_0 is relatively big (here $h = 0.001s$ and $c_0 = 50$), this approximation is precise enough:

$$\begin{cases} \dot{x}_1 = x_2 \\ \dot{x}_2 = -2x_2/c_0h - 2(x_1 - v)/(c_0h)^2 \end{cases} \quad (16)$$

Substituting signal (13) into (16), the differential equation corresponding to system (16) is gotten as follows:

$$\ddot{x}_1 + \sqrt{2}\omega_0\dot{x}_1 + \omega_0^2x_1 = \omega_0^2A \sin(\omega t) \quad (17)$$

where $\omega_0 = \sqrt{2}/c_0h$. The solution is:

$$\begin{aligned} x_1(t) &= e^{-\sqrt{2}\omega_0 t/2} \left(c_1 \cos \sqrt{2}\omega_0 t/2 + c_2 \sin \sqrt{2}\omega_0 t/2 \right) \\ &\quad + \frac{-\sqrt{2}A\omega_0^3\omega}{\omega_0^4 + \omega^4} \cos \omega t + \frac{A\omega_0^2(\omega_0^2 - \omega^2)}{\omega_0^4 + \omega^4} \sin \omega t \end{aligned} \quad (18)$$

The item with factor $e^{-\sqrt{2}\omega_0 t/2}$ attenuates quickly, so the steady state solution is written as follows:

$$\begin{aligned} \bar{x}_1 &= -\frac{\sqrt{2}A\eta}{1+\eta^4} \cos \omega t + \frac{A(1-\eta^2)}{1+\eta^4} \sin \omega t \\ &= \frac{A}{\sqrt{1+\eta^4}} \left(\frac{1-\eta^2}{\sqrt{1+\eta^4}} \sin \omega t - \frac{\sqrt{2}\eta}{\sqrt{1+\eta^4}} \cos \omega t \right) \quad (19) \\ &\approx A \sin(\omega t - \varphi) \end{aligned}$$

where,

$$\eta = \omega / \omega_0 \ll 1 \quad (20)$$

$$\begin{aligned} \varphi &= \tan^{-1} \left(\sqrt{2}\eta / (1 - \eta^2) \right) \approx \sqrt{2}\eta \\ &= \sqrt{2}\omega / \omega_0 = \omega c_0 h \end{aligned} \quad (21)$$

Substituting Eq. (21) into (19), we get:

$$\bar{x}_1 \approx A \sin \omega(t - \tau), \tau = c_0 h \quad (22)$$

According to the analysis above, when the frequency band of the input signal is much lower than the limit $\omega_0 = \sqrt{2}/c_0h$, the nonlinear TD can achieve its best filtering performance, the approximate time delay is $\tau = c_0h$ and the amplitude attenuation is small enough to be ignored.

In engineering practice, the train's acceleration and its change rate are limited, so the acceleration

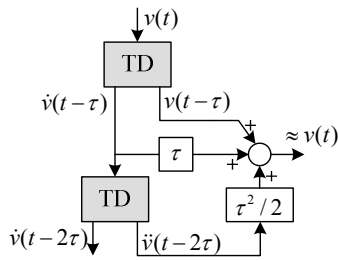
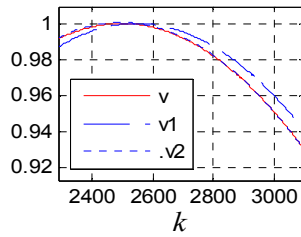
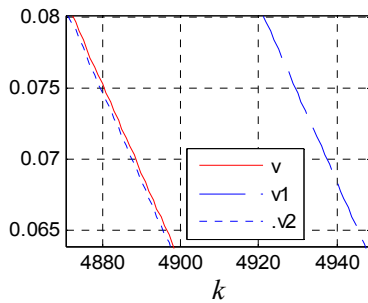


Fig. 8: Time delay compensation algorithm



(a)



(b)

Fig. 9: Compensation results

increment in time span τ can be ignored. Thus, we have the time delay compensation algorithm as follows:

$$v(t) \approx v(t-\tau) + \dot{v}(t-\tau)\tau + \frac{1}{2}\ddot{v}(t-2\tau)\tau^2 \quad (23)$$

The algorithmic realization of (23) is shown in Fig. 8.

The stimulation results of the time delay compensation algorithm are shown in Fig. 9. Where, the input signal is $v(k) = \sin(0.2\pi t)$, $h = 0.001$ and $c_0 = 50$. v_1 is the state $x_1(k)$ of TD (6), v_2 is the compensated signal and k is simulation step number.

FILTERING TIME DELAY COMPENSATION EXPERIMENTS

The experiments is carried out on a 1.5 km test line in shanghai. DSP TMS320LF2407 is chosen as the

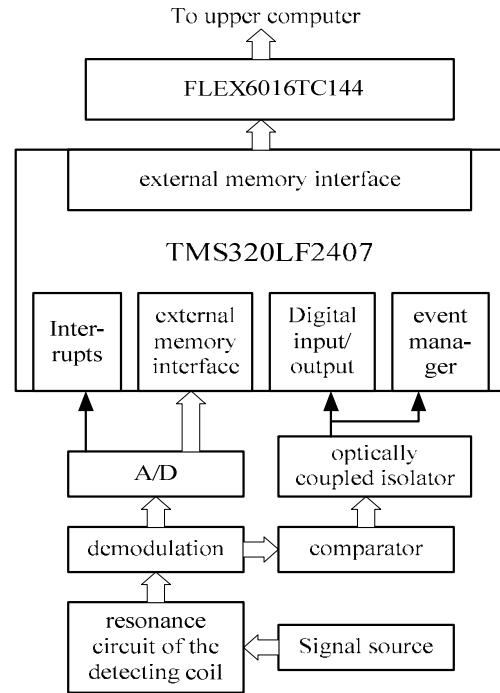


Fig. 10: Hardware structure of the sensor

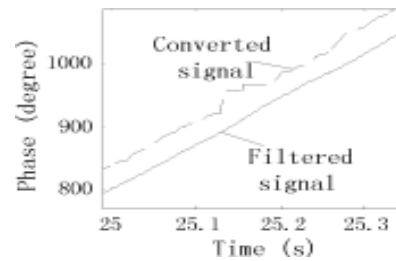


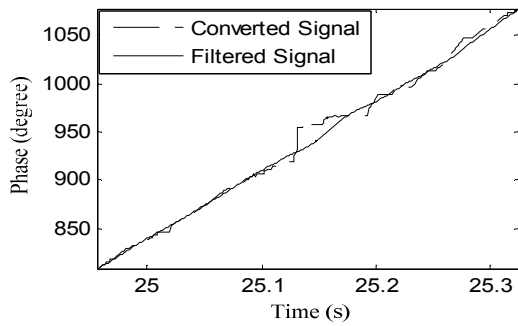
Fig. 11: Converted signal and filtered signal

processor of the sensor. FPGA FLEX6016TC144 is used to implement the communication protocol between the sensor processor and the upper computer. The block diagram of the hardware structure of the sensor is shown in Fig. 10.

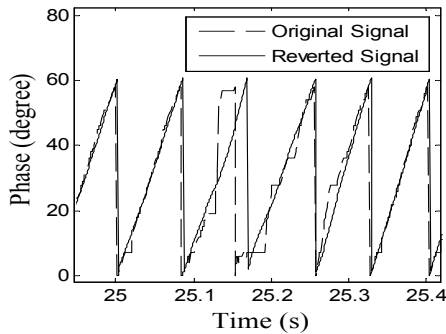
The jumping edges of the phase signal shown in Fig. 5b contain high frequency components. Filtering the phase signal straightforwardly will cause seriously information loss. So, at first, the phase signal needs to be converted to a certain form suitable for filtering. Let $ph(k)$ denote the current phase value and $n(k)$ denote the current tooth-slot period number. Considering a tooth-slot period is corresponding to a phase angle of 60° , the converted signal is calculated as follows:

$$ph_c(k) = 60n(k) + ph(k) \quad (24)$$

Because of the slight time difference between the jumping edges of the phase signal and those of the



(a)



(b)

Fig. 12: (a) Converted signal and filtered signal, (b) reverted signal and original signal

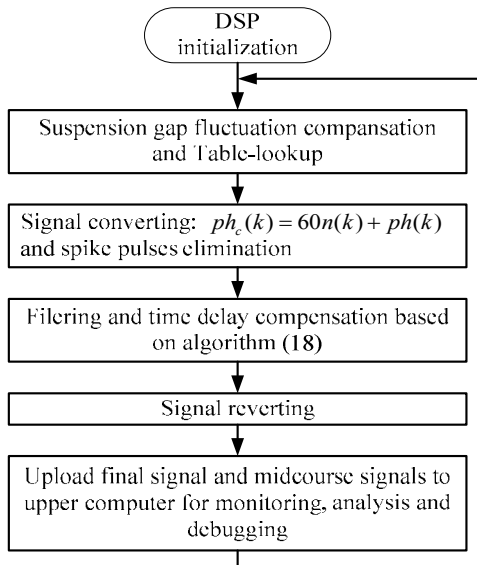


Fig. 13: Program flowchart of the sensor

tooth-slot number signal, there are spike pulses in signal $ph_c(k)$. The spike pulses can be eliminated though simple logical pretreatment.

The converted signal and the filtered signal without time delay compensation are shown in Fig. 11, where, $c_0 = 50$ and $r = 500000$. It can be seen that although the filtered signal is smooth enough, the time delay is apparent and positioning error will be caused accordingly.

The filtering results after compensation are shown in Fig. 12, where the values of c_0 and r are the same with Fig. 11. It can be seen that the time delay compensation algorithm is effective.

The program flowchart of the sensor is shown in Fig. 13.

CONCLUSION

The phase filtering technique for maglev train based on nonlinear TD is introduced. Considering the time delay characteristic of the nonlinear TD, a compensation algorithm with relatively small computation needs is proposed based on the analysis results of the dynamic performance of the nonlinear TD. The effectiveness of the algorithm designed is proved through experiments.

ACKNOWLEDGMENT

This study is supported by National Natural Science Foundation of China (No. 60974128).

REFERENCES

- Barandiaran, J.M. and G.V. Kurlyandskaya, 2009. Multilayer magnetoimpedance sensor for nondestructive testing. *Sens. Lett.*, 7: 374-377.
- Liu, H.Q., 1995. *Transrapid*. University of Electronic Sience and Technology of China Press, Chengdu, China.
- Long, Z.Q., G. He and S. Xue, 2011a. Study of EDS and EMS hybrid suspension system with permanent-magnet halbach array. *IEEE T. Magn.*, 47: 4717-4724.
- Long, Z.Q., G. He, N. He and Z.Z. Zhang, 2011b. Experimental research on an energy-saving maglev train. *Environ. Eng. Manag. J.*, 10: 19-23.
- Thomas, V., P.Y. Joubert and E. Voure'h, 2009. Study for the design of an eddy current array probe for the imaging of aeronautical fastener holes. *Sens. Lett.*, 7: 460-465.
- Wu, X.M., 2003. *Maglev Train*. Shanghai Science and Technology Press, Shanghai, China.